NASA Technical Memorandum 85768

USAAVSCOM TECHNICAL REPORT TR-84-B-2

INTERLAMINAR FRACTURE OF COMPOSITES

T. KEVIN O'BRIEN

JUNE 1984

NASA
National Aeronautics and Space Administration

Langley Research Center
Hampton Virginia 23665

U.S. ARMY
AVSCOM

SUMMARY

Fracture mechanics has been found to be a useful tool for understanding composite delamination. Analyses for calculating strain energy release rates associated with delamination growth have been developed. These analyses successfully characterized delamination onset and growth for particular sources of delamination. Low velocity impact has been found to be the most severe source of composite delamination. A variety of test methods for measuring interlaminar fracture toughness are being developed to identify new composite materials with enhanced delamination resistance.

INTRODUCTION

As high strength, low density fiber reinforced polymer matrix composites are considered for highly strained primary aircraft structures, increased attention is being devoted to the understanding and characterization of significant composite failure modes. Perhaps the most commonly observed failure mode in composites is delamination, which is a separation of the individual plies. Delamination may result from low velocity impact, from eccentricities in structural load paths that induce out-of-plane loads, or from discontinuities in the structure which create local out-of-plane loads. Because delamination occurs so frequently, interest in analyzing and characterizing delamination behavior has increased. Fracture mechanics has been found to be a useful tool for this purpose. Summaries of some of the significant recent studies on delamination are included in this review.

A Perspective

There is a fundamental difference between the way linear elastic fracture mechanics is being applied to delamination in composites and the way it is used for metals. In metals, the largest crack in a component is assumed to

control strength. Failure of the structure may be directly related, by the material's fracture toughness, to catastrophic propagation of this crack. However, composite delamination in structures subjected to in-plane loading is a subcritical failure mode whose effect may be (1) a stiffness loss that is benign in terms of the structural failure, (2) a local tensile strain concentration in the load bearing plies that causes tensile failure, or (3) a local instability that causes further growth which ends in compressive failure. In the latter two cases the delamination leads to a redistribution of structural load paths which, in turn, precipitates structural failure. Hence, delamination is indirectly responsible for the final failure of a composite, whereas crack propagation in a metal is directly responsible for structural failure. Consequently, interlaminar fracture toughness for composite delamination does not have the same significance to design as fracture toughness does for a metal. The designer must be able to determine the consequence of the delamination in terms of structural load redistribution and relate this to some appropriate structural failure criterion. Nevertheless, fracture mechanics is a useful tool for understanding the mechanics of delamination, to determine the variables that control when delaminations form and grow, and for characterizing the inherent delamination resistance of the composite. This paper will focus on these aspects of the fracture mechanics characterization of delamination in composite materials.

MECHANICS OF DELAMINATION

Strain Energy Release Rate Analysis

Some potential delamination sites are the common design details that result in discontinuities in the load path. These discontinuities give rise to interlaminar stresses even when the remote loading is in-plane [1]. Some of these typical design details (fig. 1) are (1) a straight edge with a

stress-free boundary (often called a "free edge"), (2) a curved edge such as a hole boundary, (3) a drop off of the interior plies of a laminate to taper thickness, (4) a bonded or co-cured joint, and (5) a bolted joint. Of these cases, the free-edge delamination problem has been studied most extensively, and illustrates the benefits of fracture mechanics for characterizing delamination behavior.

Several investigators have analyzed the strain energy release rate, G, associated with edge delamination growth [2,3,4]. From finite element analysis they have found that once the delamination progresses beyond a distance equal to a few ply thicknesses from the edge, G reaches a constant plateau given by the first equation in figure 2. This equation, derived from a rule of mixtures and laminated plate theory, shows that G is independent of delamination size and depends only on the remote strain, ε, the laminate thickness, t, and two modulus terms, E_{LAM} and E^*, that correspond to the laminate modulus before and after delamination. In Reference [4], the critical strain, ε_c, measured at the onset of edge delamination in the -30/90 interfaces of eleven-ply $[\pm 30/\pm 30/90/\overline{90}]_s$ laminates was substituted into the edge delamination equation in figure 2 to determine a critical G_c for Thornel 300/Narmco 5208* (graphite/epoxy) composites. This G_c was then used to predict onset strains for edge delamination in the 0/90 interfaces of $[+45_n/-45_n/0_n/90_n]_s$ laminates of the same material, where n = 1,2,3 corresponded to and 8-, 16-, and 24-ply laminate. Figure 3 shows that the predictions agreed well with experimental data, and captured the trend of decreasing delamination onset strain with increasing thickness. An analysis based on critical values of interlaminar stresses would not account for this thickness dependence because the interlaminar stresses are independent of n [3]. No rigorous analytical explanation has been presented to explain the ability of the strain energy

*The use of trade names in this article does not consitute endorsement, either expressed or implied, by the National Aeronautics and Space Administration or AVSCOM.

release rate (which is rigorously defined only when a crack of finite size exists) to predict delamination onset when a stress criterion cannot. Although the interlaminar stresses in the interfaces that delaminate are singular at the straight edge, these singularities are not the same as those that exist when the delamination has formed [5,6]. Perhaps the most logical explanation is the presumption that inherent interlaminar flaws of microscopic dimension are initially present in the interface near the edge, or they are created by the singular stresses at the edge, but they do not form delaminations of a finite detectable size until a critical G value is reached for delamination extension [4,7,8].

A similar analysis for a local delamination growing from a matrix ply crack in an off-axis ply yielded the second equation shown in figure 2 [9]. This equation also shows that G is independent of delamination size and depends only on the remote load, P, the laminate width, W, the laminate thickness, t, the laminate modulus, E_{LAM}, and the thickness and modulus of the uncracked, locally delaminated regions, t_{LD} and E_{LD}, respectively. Figure 4 shows predictions (open symbols) of delamination onset in the -25/90 interfaces of $[\pm 25/90_n]_s$ laminates. Under tensile loading, these laminates undergo a transition from edge delamination ($n < 3$) to local delamination growing from matrix cracks ($n > 4$). A critical G_c was calculated from the $n = 2$ edge-delamination data, and then was substituted into the appropriate equations to predict delamination onset strains for the other layups. As shown in figure 4, the G anlyses predict the onset of both types of delamination well. Furthermore, just as the dependence for edge delamination was predicted by G analysis (fig. 3), so the trend of decreasing ε_c with increasing thickness of the cracked ply, and hence increasing n, was predicted for local delamination (fig. 4).

The ability of the strain energy release rate to correlate delamination behavior from several sources and account for volumetric effects in the form of thickness dependence is the primary reason for adopting fracture mechanics to analyze delamination problems. Historically, this same capability for predicting crack growth in large metallic structures based on fracture toughness measurements of small test specimens led to the acceptance and growth of fracture mechanics in the 1950's [10].

Mixed-Mode Behavior

Because a delamination is constrained to grow between individual plies, both interlaminar tension and shear stresses are commonly present at the delamination front. Therefore, delamination is often a mixed-mode fracture process. A boundary value problem must be formulated and solved to determine the G_I, G_{II}, and G_{III} components of the total strain energy release rate. A virtual crack extension technique has been combined with displacement-based finite element analysis to calculate the various G components [2]. This technique, in conjunction with quasi-three-dimensional finite element analyses, was applied to the free-edge delamination problem by several authors [2,3,4,7,11,12,13]. Figure 5 shows the results of such an analysis for the $[\pm 30/\pm 30/90/\overline{90}]_s$ laminate when each of the -30/90 interfaces are assumed to delaminate. As noted earlier, the total G raises to a constant plateau when the delamination progresses beyond a few ply thicknesses from the edge. Figure 5 indicates that the total G is equal to the sum of G_I and G_{II} components. The G_{III} component calculated was negligible. Furthermore, like the total G, the G_I and G_{II} components are also independent of delamination size for edge delamination.

Similar analyses have been performed for other composite layups [3,11,12,13]. Figure 6 shows the G_I percentage of the total G for three

quasi-isotropic layups containing ±45°, 0°, and 90° plies. Each layup had 90° plies in the center, but the order of the +45°, -45°, and 0° plies was permutated. Delaminations were modeled between the 90° plies and adjacent angle plies. The total G was nearly identical for the three layups but, as shown in figure 6, the G_I component varied significantly.

Because of the complex mixed-mode nature of composite delamination, no closed form solutions have been developed to lay a strong theoretical foundation for understanding the governing parameters that control delamination behavior. Recently, however, a singular integral equation approach based on anisotropic composite laminate elasticity theory was used to establish some general asymptotic solutions for edge delamination [14]. A partially closed crack model for delamination was introduced to remove the restriction of physically inadmissible oscillatory stress singularities. Both the global response in terms of strain energy release rates (G_I, G_{II}, G_{III}, and G_{TOTAL}) and the asymptotic field solution in terms of crack-tip stress intensity factors (K_I, K_{II}, and K_{III}) were calculated. Anisotropic laminate elasticity solutions were obtained for relatively simple cases of delamination in $(+\theta/-\theta)_s$ laminates [14]. Finite element methods based on a combined laminate elasticity solution and singular hybrid finite element formulation were employed for fiber composites with complex lamination variables [15]. Figure 6 shows the G_I percentage of the total G for edge delamination in the $(\pm 45/0/90)_s$ family analyzed previously. The same trend in G_I/G with layup is apparent, indicating that the simple approximate techniques, used with the more common displacement-based finite elements, may be reasonably accurate for predicting delamination behavior. The virtual crack extension method has been successfully used with a 3D NASTRAN finite element analysis to

predict delamination growth from both a manufacturing flaw and an oper hole in the F-16 composite horizontal tail [1].

The fracture mechanics analyses of other sources of delamination will continue to be a fruitful research topic as composite materials become candidates for primary aircraft structure. Both the U.S. Air Force and the U.S. Army are developing damage tolerance and durability criteria for future composite structures which may ultimately require such analyses for structural certification.

DELAMINATION GROWTH

Delaminations in composite laminates may interact with other damage mechanisms that result in different growth behavior than may be anticipated from an elastic analysis. For example, under quasi-static loading, edge delamination formation is followed by matrix cracking in the 90° plies. These matrix cracks may extend throughout the laminate width, ahead of the delamination front [4], causing a perturbation in the three-dimensional stress field at the delamination front. This interaction between matrix cracks and delamination causes stable delamination growth. A two-dimensional linear elastic fracture mechanics analysis cannot model this three-dimensional damage, but it may be used for semi-empirical characterization of stable growth using the R-curve method [16]. Figure 7 shows an R-curve for stable edge delamination growth in a $[\pm 45/0/90]_s$ T300/5208 laminate [17]. Unlike the G predicted from an elastic analysis that is independent of delamination size, a, the delamination resistance, G_R, increases with a as the matrix cracking accumulates ahead of the delamination front. As shown in figure 8, this R-curve was used to predict stable edge-delamination growth in a thicker $[+45_2/-45_2/0_2/90_2]_s$ laminate, and in a $[\pm 30/\pm 30/90/\overline{90}]_s$ laminate with a different layup.

If the composite has a tough matrix, however, the matrix cracking may be suppressed. Delaminations will form at higher G values, but they will immediately extend through the laminate width in an unstable manner [7]. This edge delamination behavior in a toughened-matrix composite is the opposite of the stable crack growth observed in a ductile metal where large plastic zones at the crack tip result in more stable growth.

Another source of delamination resistance that results in stable growth is the fiber bridging that occurs when a delamination is forced to grow between plies of similar orientation. This often occurs in the double cantilever beam (DCB) test used to measure Mode I interlaminar fracture toughness [18,19,20]. Figure 9 shows the DCB specimen, which typically consists of 24 plies of unidirectional material. As shown on figure 9, the specimen compliance is a non-linear function of delamination size. In reference [20], a Teflon* coated glass fabric was placed at the midplane in the end of the beam to simulate a crack-like sharp notch. Measurements of G_{Ic} were taken at the initial insert length (delamination length = 0) and along the length of the beam as the delamination grew. Figure 10 shows the R-curve generated from a DCB specimen of Hercules HMS/3501-6* (graphite/epoxy). The three-fold increase in G_{Ic} from the initiation at the crack starter until values stabilized after the delamination grew over one third of the beam legnth was attributed to fibers debonding from the matrix, bridging the delamination plane, flexing, and breaking. A similar R-curve generated for an Hercules AS-1/3501-6* DCB specimen showed a higher G_{Ic} at initiation and less increase in G_{Ic} as the delamination grew (fig. 10). In this case, much less fiber bridging was observed due to the stronger interfacial bond between the AS-1 fiber and the 3501-6 matrix.

Unlike the stable delamination growth that occurs under quasi-static loading at G levels above G_c, cyclic delamination growth may occur at

levels well below the static interlaminar fracture toughness. Figure 11 shows results for cyclic edge delamination tests at maximum cyclic strain levels below the delamination onset strain measured in the static test [11]. Delaminations formed at these lower cyclic strains after a certain number of cycles, N. G_c values, calculated from maximum cyclic strains and plotted as a function of the number of cycles to delamination onset, are shown in figure 11. These G_c values drop sharply in the first 200,000 cycles until they reach a plateau tantamount to a threshold for delamination onset in fatigue. An elastic analysis of the $[\pm 35/0/90]_s$ and $[0/\pm 35/90]_s$ laminates yields an identical total G for a given nominal strain, but their G_I components are very high and low, respectively. As shown in figure 11, the G_c for these two layups measured in static tests (N = 0) are different. However, the G_c thresholds under cyclic loading are nearly identical. Hence, the total G does not determine the delamination onset under static loading, but does appear to govern the delamination onset in fatigue. Furthermore, comparison of the relatively tough Hexcel HX205 matrix composites to the brittle 5208 matrix composite shows a significant improvement in the static G_c, yet the magnitude of this improvement for the G_c threshold in fatigue is much less.

The comparisons shown in figure 11 are useful for selection of more durable composite matrices. However, for damage tolerance analysis, a complete characterization of delamination growth, from the onset threshold under cyclic loading, G_{th}, to the static interlaminar fracture toughness, G_c, is required (fig. 12). Several investigators have used the mode I DCB and mixed-mode cracked-lap-shear (CLS) specimens to characterize this delamination growth [1,21,22,23]. They have developed delamination growth laws of the form $\frac{da}{dN} = cG^b$ similar to cyclic crack growth laws used to characterize fatigue

crack growth in metals. These baseline data were used with finite element analyses to predict cyclic delamination growth in structural components [1].

One source of composite delamination growth is the local instability that arises from the buckling of a delaminated region under compression loading [24,25]. Figure 13 shows a comparison of measured delamination cyclic growth rates, da/dN, and strain energy release rate components, G_I and G_{II}, calculated from a geometrically nonlinear finite element analysis for a compressively loaded laminate containing a through-width delamination [25]. Both G_I and the delamination growth rate increase and then decrease rapidly with delamination extension. However, G_{II} increases monotonically to a constant level with delamination extension. Hence, it appears that G_I is primarily responsible for driving the delamination in the buckled region, even though the G_{II} component was an order of magnitude larger.

Figure 13 also shows the tendency for the delamination cyclic growth rate to decrease with delamination length. Hence, the growth of a single delamination under cyclic compression may arrest and hence may not severely degrade performance. Figure 14 shows plots of cycles to failure as a function of maximum cyclic strain for a 38-ply T300/5208 (graphite/epoxy) laminate, typical of an upper surface transport wing skin, subjected to cyclic compressive loading [26] where (1) the laminates contain a single circular insert, of various diameters, located at different interfaces to simulate delamination, (2) the laminates have been subjected to low velocity impacts over a range of impact energies, and (3) the laminate contains a 1.27 cm (0.5 in) diameter hole. The impacted laminates suffered severe degradation in the compressive strain at failure. In most cases the static compressive failure strain after impact was less than the residual compressive strain for the implanted delamination after 10^6 fatigue cycles.

Figure 15 shows a plot of cycles to failure as a function of stress amplitude for $[0/90/0/\pm45/0]_s$ graphite epoxy laminates subjected to fully reversed cyclic loading, either in the undamaged state, or following an impact with a potential energy per unit thickness of 1790 J/m [27]. All failures occurred in the compression cycle. The data in figure 15 indicate that the compressive strength after impact is very low compared to the fatigue behavior of the virgin laminate. Furthermore, most of the strength reduction occurs after the impact, with very little degradation due to subsequent cyclic loading.

The results in figures 14 and 15 indicate that, unlike metals where cyclic loading poses the most severe threat of crack growth leading to failure, the most severe source of delamination in graphite epoxy structural laminates is low velocity impact. Such impacts may create significant delamination throughout the thickness of the laminate, degrading compressive strength. Furthermore, this extensive delamination may occur on the laminate interior with little or no visible damage apparent on the laminate surface [26-30]. Some research has just begun to relate the strain energy release rate for delamination growth due to out-of-plane loading during impact to the growth of multiple delaminations that form throughout the laminate thickness. One analysis is based on large deflection plate theory for circular isotropic plates containing multiple delaminations [31]. The influence of plate thickness, support conditions, and matrix toughness on the onset and propagation of delamination was predicted. Figure 16 shows a comparison of the predicted and measured load-displacement record for a 16-ply, circular quasi-isotropic plate, 25 mm in diameter, subjected to a transverse load. Seven symmetrically loaded delaminations were assumed to grow simultaneously. Good agreement was found for the initial delamination onset at a load of 1 kN, and for the

load-displacement curve, up to the point that fiber breakage occurred in the back surface ply, at a load of 3 kN. More refined analyses that model the specific damage details observed during low velocity impact are needed to further clarify the relationships between impact loading and interlaminar fracture.

CHARACTERIZATION OF DELAMINATION RESISTANCE

Because of this severe delamination threat posed by non-visible, low velocity impact, there has been increased interest in developing new toughened matrix resins for graphite reinforced composites. Several investigators have identified a correlation between improved compressive strength after impact and improved interlaminar fracture toughness for compositses with toughened matrix resins [26,29,30]. These observations provided motivation for developing new test methods for measuring interlaminar fracture toughness.

Many investigators have used a double cantilever beam (DCB) specimen (fig. 9) to measure critical values of the crack opening (interlaminar tension) fracture toughness, G_{Ic} [18-23,32-34]. The edge delamination test (EDT) (fig. 17) is also being used to measure the mixed-mode fracture toughness of composites [7] and determine fracture mode dependence [35,-36]. Figure 18 shows a comparison of the interlaminar fracture toughness of graphite composites with very brittle or tough matrix resins tested using a 24-ply unidirectional DCB as well as three EDT layups with low, intermediate, and high percentages of G_I. The solid symbols represent mode I component of measured G_c. Results indicated that only the G_I component controlled interlaminar fracture for the brittle matrix composites (5208, 2202-1)* whereas both interlaminar tension and shear contributed to delamination in tough matrix composites (HX205/P1o5)*. Both the DCB and EDT tests are being used to evaluate new composite materials developed for heavily loaded large composite wing skins under the NASA Aircraft Energy Efficiency (ACEE) project [37].

Several other tests are also being used to measure interlaminar fracture toughness. A pure mode I version of the EDT test has been proposed [38]. The cracked-lap shear-(CLS) test for mixed mode G_c has been used by several investigators [19,21,22]. Currently an ASTM task group is conducting a round robin test program using the DCB, EDT, and CLS specimen as a prelude to developing ASTM standards. Other investigators have used unidirectional beams loaded in three-point bending to estimate G_{IIc} [19,39,40,41] or loaded asymmetrically to measure mixed mode G_c values with different ratios of G_I/G_{II} [19,40].

The recognition of the importance of interlaminar fracture toughness to composite damage tolerance has led to the development of new toughened matrix composites. Because resin manufacturers would prefer to measure the fracture toughness of a small neat resin specimen, there has been renewed interest in composite micromechanics analyses. The ultimate goal of such analyses would be to relate the fracture behavior of the neat resin to the interlaminar fracture behavior of the composite. Such analyses would guide the development of neat resin fracture tests that would yield realistic estimates of improvements in interlaminar fracture toughness of composites.

CONCLUSIONS AND FUTURE DIRECTIONS

Although the promise of composite materials has been known for several decades, the application of these materials to primary aircraft structure is just beginning. As suitable toughened-resin composites are developed to overcome the existing impact problems, methods for characterizing their behavior will have to be re-evaluated. For example, it may become necessary to use a J-integral analysis to correlate delamination behavior between

different layups and structural discontinuities. Furthermore, fatigue may reappear as the limiting factor for damage tolerant design. In any event, the ability to anticipate and quantify delamination failure using fracture mechanics analyses will still play an important role in the understanding of composite behavior, in establishing the damage tolerance and durability design criteria for certification, and in the development of improved composite materials.

REFERENCES

[1] Wilkins, D. J., "A Preliminary Damage Tolerance Methodology for Composite Structures," in Failure Analysis and Mechanisms of Failure of Fibrous Composite Structures, NASA CP 2278, 1983, pp. 67-93.

[2] Rybicki, E. F., Schmueser, D. W., and Fox, J., Journal of Composite Materials, vol. 2, 1977, p. 470.

[3] Crossman, F. W., Warren, W. T., Wang, A. S. D., and Law, G. E., "Initiation and Growth of Transverse Cracks and Edge Delamination in Composite Laminates." J. of Composite Materials, Supplemental Volume (1980), pp. 88-106.

[4] O'Brien, T. K., "Characterization of Delamination Onset and Growth in a Composite Laminate," in Damage in Composite Materials, ASTM STP 775, June 1982, p. 140.

[5] Wang, S. S., and Choi, I., "Boundary-Layer Effects in Composite Laminates: Part 1 - Free Edge Stress Singularities," J. of Applied Mechanics, vol. 104, Sept. 1982.

[6] Wang, S. S., and Yuan, F. G., "A Hybrid Finite Element Appr ch to Composite Laminate Elasticity Problems With Stress Singularities," ASME J. of Applied Mechanics, vol. 50, no. 4, Dec. 1983.

[7] O'Brien, T. K., Johnston, N. J., Morris, D. H., and Simonds, R. A., "A Simple Test for the Interlaminar Fracture Toughness of Composites," SAMPE Journal, vol. 18, no. 4, July/August 1982, p. 8.

[8] Wang, A. S. D., and Slomiana, M., "Delamination Crack in Graphite Epoxy Laminates Initiated by Compression," Presented at the ASTM Symposium on Delamination and Debonding of Materials, Pittsburgh, PA, Nov. 1983.

[9] O'Brien, T. K., "Analysis of Local Delaminations and Their Influence on Composite Laminate Behavior," NASA TM 85728, January 1984 (Presented at the ASTM Symposium on "Delamination and Debonding of Materials," Pittsburgh, PA, November 1983).

[10] Irwin, G. R., Seminar on the History of Fracture Mechanics, Virginia Polytechnic Institute, Blacksburg, VA, September 1982.

[11] O'Brien, T. K., "Mixed-Mode Strain-Energy-Release-Rate Effects on Edge Delamination of Composites," in "The Effect of Defects in Composite Materials," ASTM STP 836, 1984. Also in NASA TM-84592, January 1983.

[12] Whitcomb, J. D., and Raju, I. S., "Analysis of Free-Edge Stresses in Thick Composite Laminates," NASA TM 85738, January 1984 (Presented at the ASTM Symposium on "Delamination and Debonding of Materials," Pittsburgh, PA, November 1983).

[13] O'Brien, T. K., Raju, I. S., and Garber, D. P., "Residual Thermal and Moisture Influences on the Strain-Energy-Release-Rate Analysis of Edge Delamination," to appear in Composites Technology Review, 1984.

[14] Wang, S. S., "Fracture Mechanics for Delamination Problems in Composite Materials," J. of Composite Materials, vol. 17, no. 3, May 1983, pp. 210-223.

[15] Wang, S. S., and Choi, I., "The Interface Crack Behavior in Dissimilar Anisotropic Composites Under Mixed-Mode Loading," ASME Journal of Applied Mechanics, vol. 50, 1983, pp. 178-183.

[16] Fracture Toughness Evaluation by R-Curve Methods, ASTM STP 527, 1973.

[17] O'Brien, T. K., "The Effect of Delamination on the Tensile Strength of Unnotched, Quasi-Isotropic, Graphite/Epoxy Laminates," Proceedings of the SESA/JSME Joint Conference on Experimental Mechanics, Part I, Hawaii, May 1982, pp. 236-243.

[18] deCharentenay, F. X., et al., "Characterizing the Effect of Delamination Defect by Mode I Delamination Test," Presented at ASTM Symposium on The Effect of Defects in Composites, San Francisco, CA, December 1982.

[19] Russell, A. J., and Street, K. N., "Moisture and Temperature Effects on the Mixed-Mode Delamination Fracture of Unidirectional Graphite Epoxy," Presented at the ASTM Symposium on Delamination and Debonding of Materials, Pittsburgh, PA, November 1983.

[20] Russell, A. J., "Factors Affecting the Interlaminar Fracture Energy of Graphite/Epoxy Laminates," In Progress in Science and Engineering of Composites; Proceedings of ICCM - IV, Tokyo, 1982, pp. 279-286.

[21] Wilkins, D. J., et al., "Characterizing Delamination Growth in Graphite-Epoxy," in Damage in Composites, ASTM STP 775, June 1982, p. 168.

[22] Ramkumar, R. L., "Characterization of Mode I and Mixed-Mode Delamination Growth," Presented at the ASTM Symposium on Delamination and Debonding of Materials, Pittsburgh, PA, November 1983.

[23] Wilkins, D. J., "Environmental Effects on Interlaminar Toughness and Subcritical Delamination Growth," Presented at the ASTM Symposium on Delamination and Debonding of Materials, Pittsburgh, PA, November 1983.

[24] Chai, H., Babcock, C. D., and Knauss, W. G., "One-Dimensional Modeling of Failure in Laminated Plates by Delamination Buckling," Int. Journal of Solids and Structures, vol. 17, no. 11, 1981, pp. 1069-1083.

[25] Whitcomb, J. D., "Finite Element Analysis of Instability-Related Delamination Growth," J. of Composite Materials, vol. 15, 1981, pp. 403-426.

[26] Byers, B. A., "Behavior of Damaged Graphite/Epoxy Laminates Under Compression Loading," NASA CR 159293, August 1980.

[27] Bishop, S. M., and Dorey, G., "The Effect of Damage on the Tensile and Compressive Performance of Carbon Fibre Laminates," in Characterization, Analysis, and Significance of Defects in Composite Materials, AGARD CP-355, April 1983.

[28] Starnes, J. H., Rhodes, M. D., and Williams, J. G., "The Effect of Impact Damage and Circular Holes on the Compressive Strength of a Graphite-Epoxy Laminate," ASTM STP 696, 1979, pp. 145-171.

[29] Williams, J. G., and Rhodes, M. D., "The Effect of Resin on the Impact Damage Tolerance of Graphite-Epoxy Laminates," ASTM STP 787, Composite Materials: Testing and Design (Sixth Conference), 1982, pp. 450-480.

[30] Carlisle, D. R., and Leach, D. C., "Damage and Notch Sensitivity of Graphite/PEEK Composite," Proceedings of the 15th National SAMPE Technical Conference, October 1983, pp. 82-93.

[31] Bostaph, G. M., and Elber, W., "A Fracture Mechanics Analysis for Delamination Growth During Impact on Composite Plates," in 1983 Advances in Aerospace Structures, Materials, and Dynamics; Proceedings of the ASME Winter Annual Meeting, pp. 133-138.

[32] Bascom, W. D., Bitner, J. L., Moulton, R. J., and Siebert, A. R., "The Interlaminar Fracture of Organic-Matrix, Woven Reinforcement Composites," Composites, vol. 11, no. 9, 1980, p. 9.

[33] Miller, A. G., Hertzberg, P. E., and Rantala, V. W., "Toughness Testing of Composite Materials," Proceedings of the 12th National SAMPE Technical Conference, vol. 12, 1980, p. 279.

[34] Whitney, J. M., Browning, C. E., and Hoogsteden, W., "A Double Cantilever Beam Test for Characterizing Mode I Delamination of Composite Materials," J. of Reinforced Plastics and Composites, October 1982, pp. 297-313.

[35] Johnston, N. J., O'Brien, T. K., Morris, D. H., and Simonds, R. A., "Interlaminar Fracture Toughness of Composites II - Refinement of the Edge Delamination Test and Application to Thermoplastics," Proceedings of the 28th National SAMPE Symposium and Exhibition, Anaheim, California, April 1983, p. 502.

[36] O'Brien, T. K., Johnston, N. J., Morris, D. H., and Simonds, R. A., "Determination of Interlaminar Fracture Toughness and Fracture Mode Dependence of Composites Using the Edge Delamination Test," Proceedings of the International Conference on Testing, Evaluation, and Quality Control of Composites, University of Surrey, Guildford, England, September 1983, pp. 223-232.

[37] Standard Tests for Toughened Resin Composites, NASA RP 1092, Original - May 1982, Revised - July 1983.

[38] Whitney, J. M., and Knight, M., "A Modified Free-Edge Delamination Specimen," Presented at the ASTM Symposium on Delamination and Debonding of Materials, Pittsburgh, PA, November 1983.

[39] deCharentenay, F. X., et al., "Fatigue Delamination in CRFP Composites: Study With Acoustic Emission and Ultrasonic Testing in Mechanics of Non-Destructive Testing," W. W. Stinchcomb, editor, Plenum Press, NY, 1980, pp. 391-402.

[40] Bradley, W. L., and Cohen, R., "Matrix Deformation and Fracture in Graphite Reinforced Epoxies," Presented at the ASTM Symposium on Delamination and Debonding of Materials, Pittsburgh, PA, November 1983.

[41] Chatterjee, S. N., Pipes, R. B., and Blake, R. A., Jr., "Criticality of Disbonds in Laminated Composites," Presented at the ASTM Symposium on the Effects of Defects in Composite Materials, San Francisco, CA, December 1983.

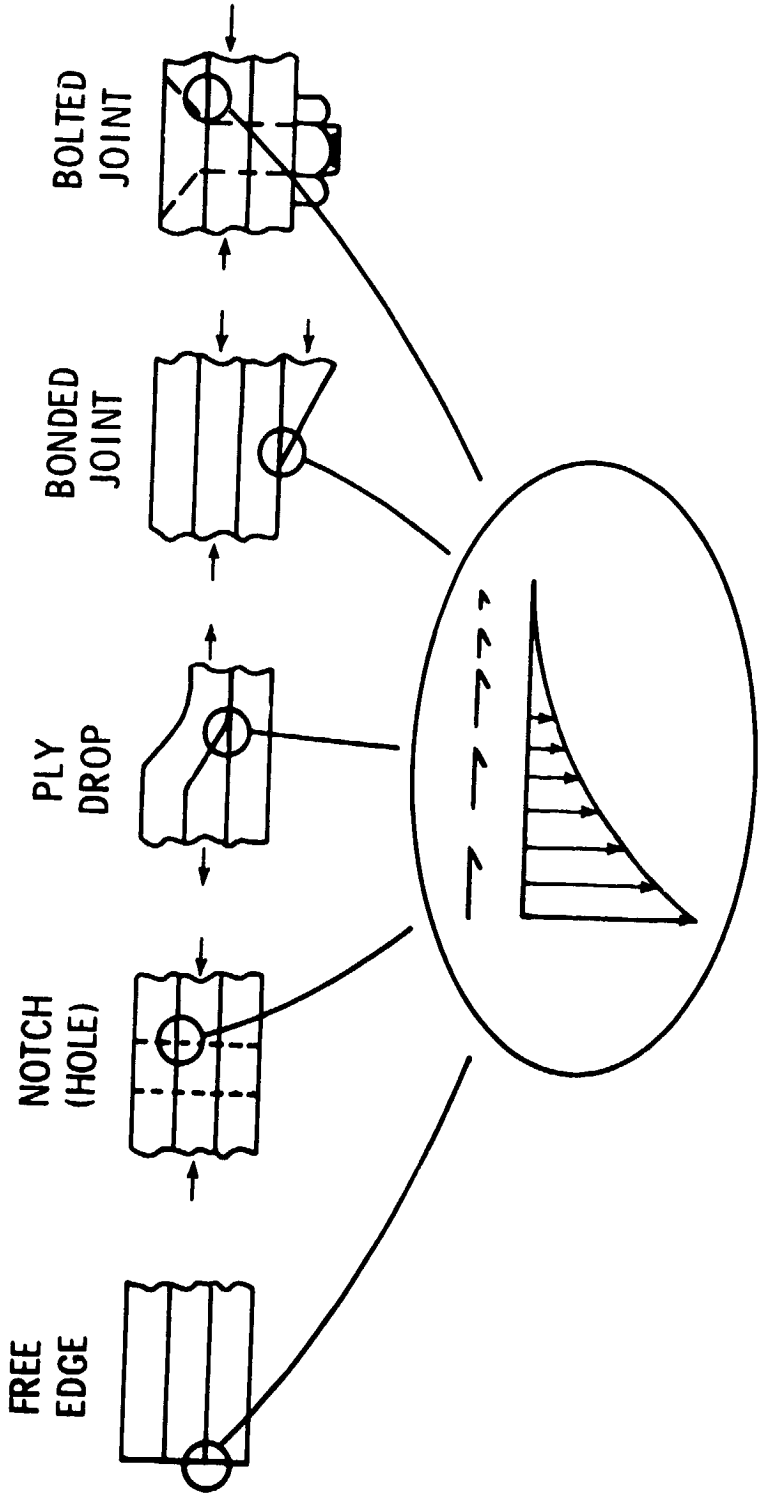

Fig 1 Sources of out-of-plane loads from load path discontinuities

EDGE
DELAMINATION

$$G = \frac{\varepsilon^2 t}{2}\left(E_{lam} - E^*\right)$$

LOCAL DELAMINATION
FROM MATRIX CRACKS

$$G = \frac{P^2}{4w^2}\left[\frac{1}{E_{LD}t_{LD}} - \frac{1}{E_{lam}t}\right]$$

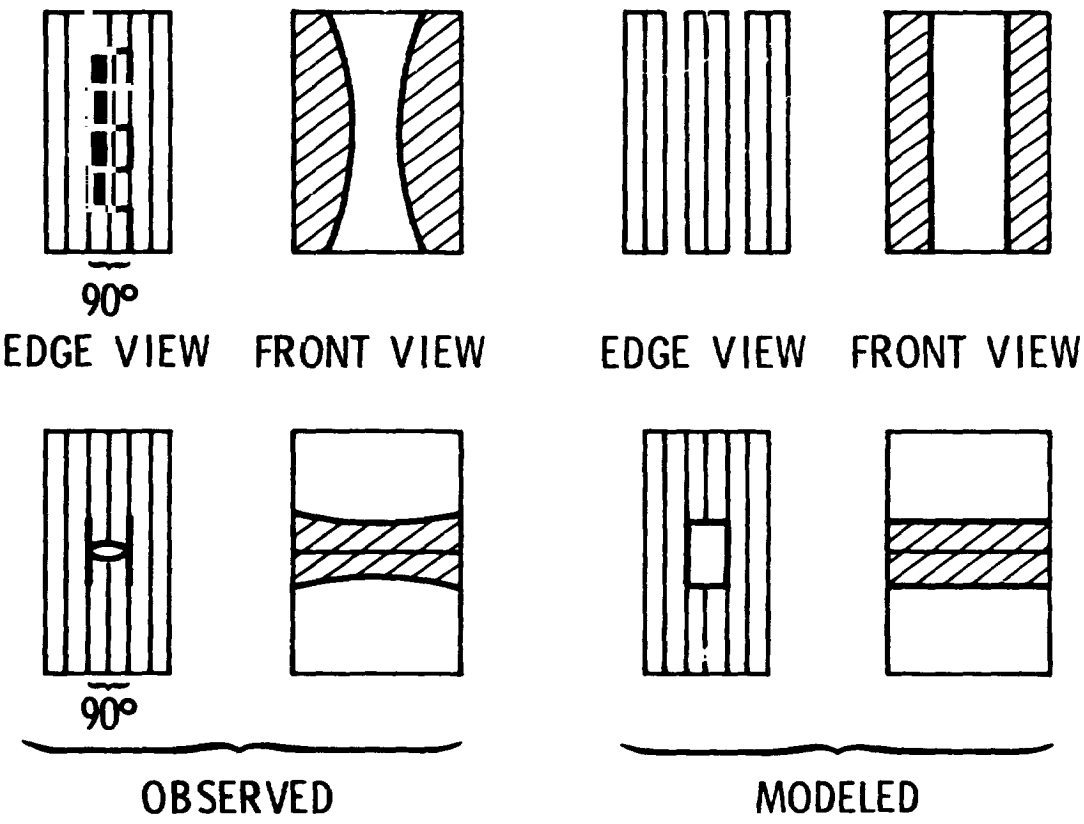

Fig 2 Sources of delamination in unnotched laminates

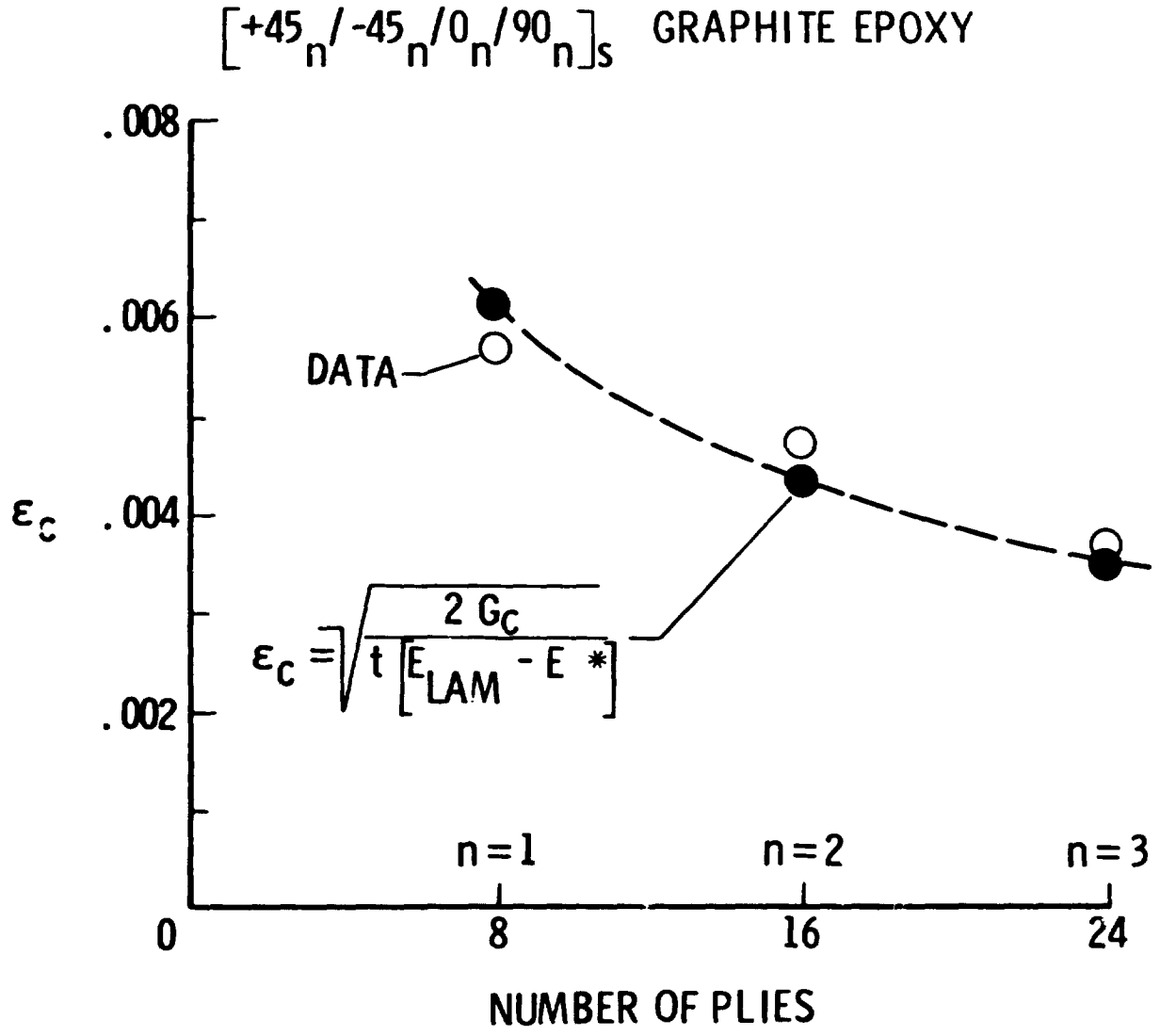

Fig 3 Edge delamination onset in 0/90 interfaces of T300/5208 laminates

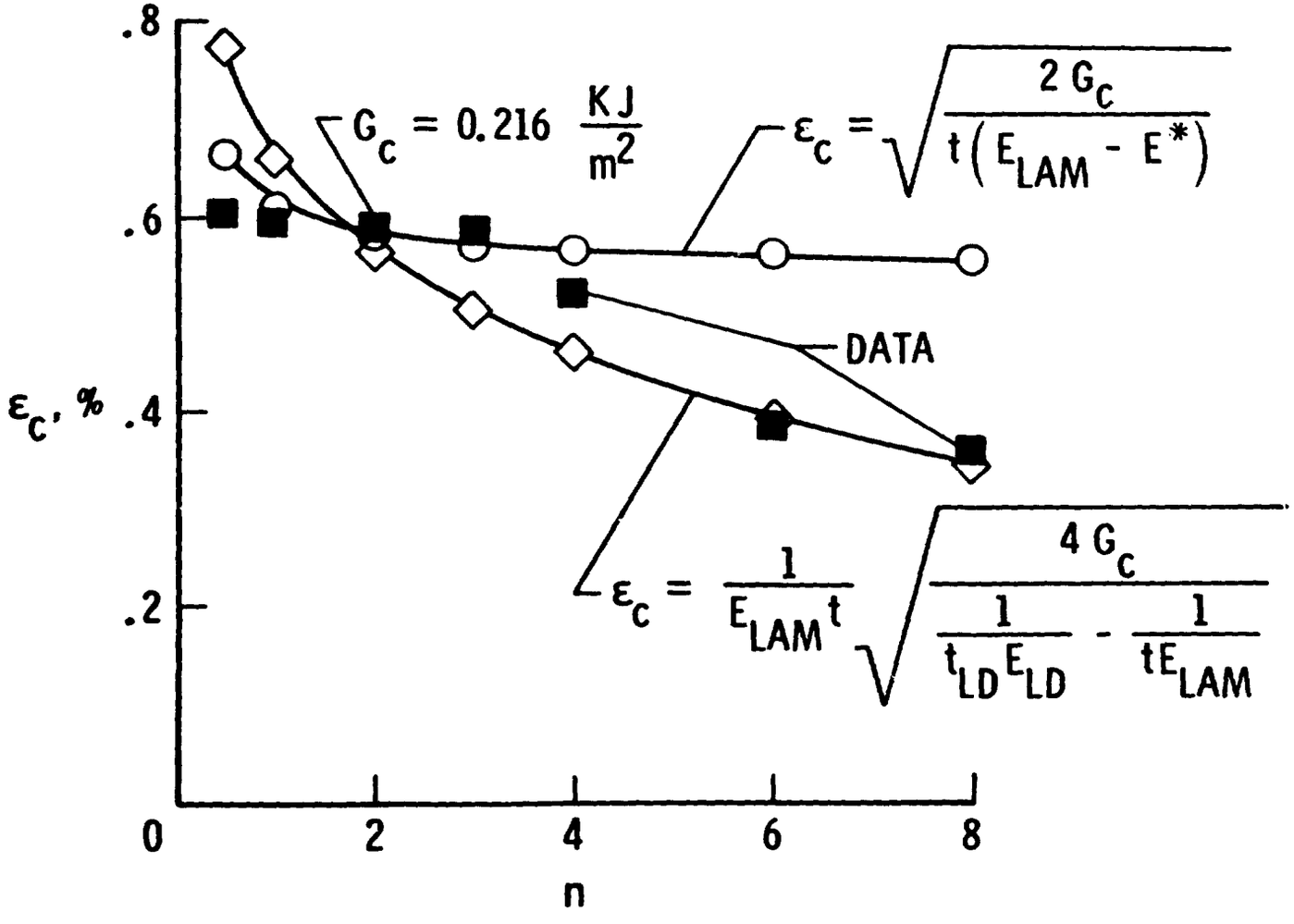

Fig 4 Prediction of delamination onset in -25/90 interfaces of $(25/-25/90_n)_s$ laminates

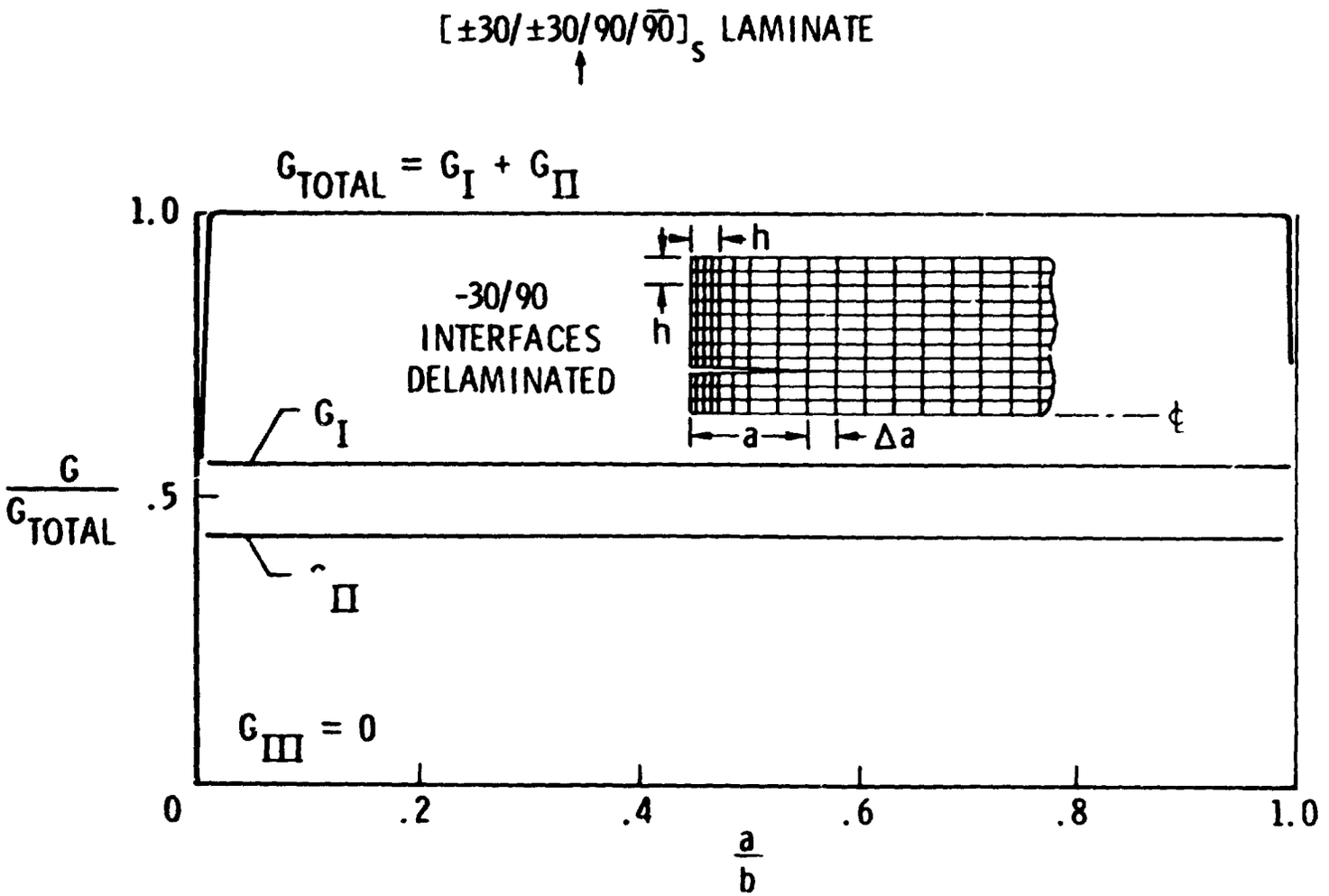

Fig 5 Strain energy release rate components for edge delamination

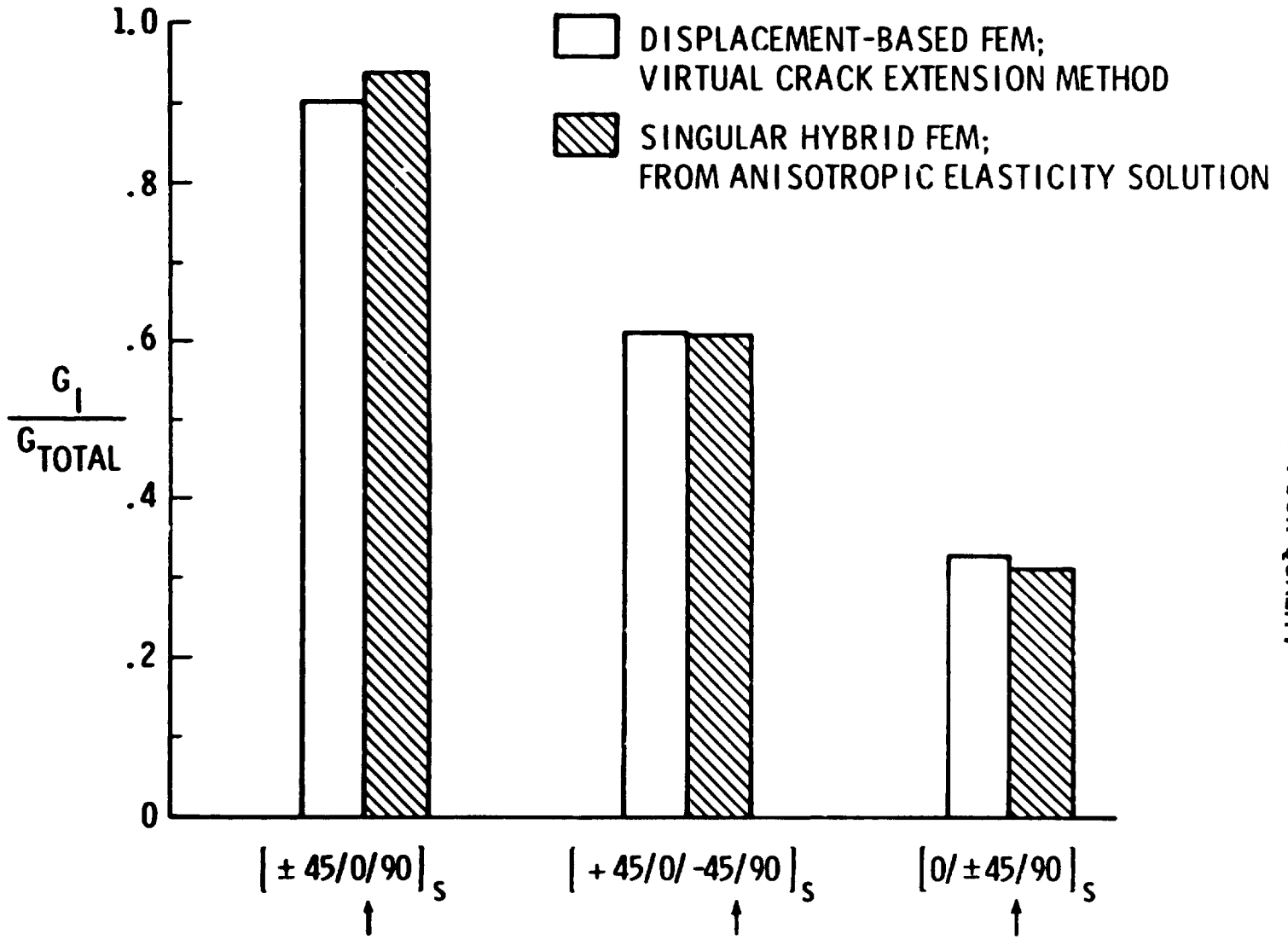

Fig 6 Mode I percentage of total G for edge delamination in θ/90 interfaces of quasi-isotropic laminates

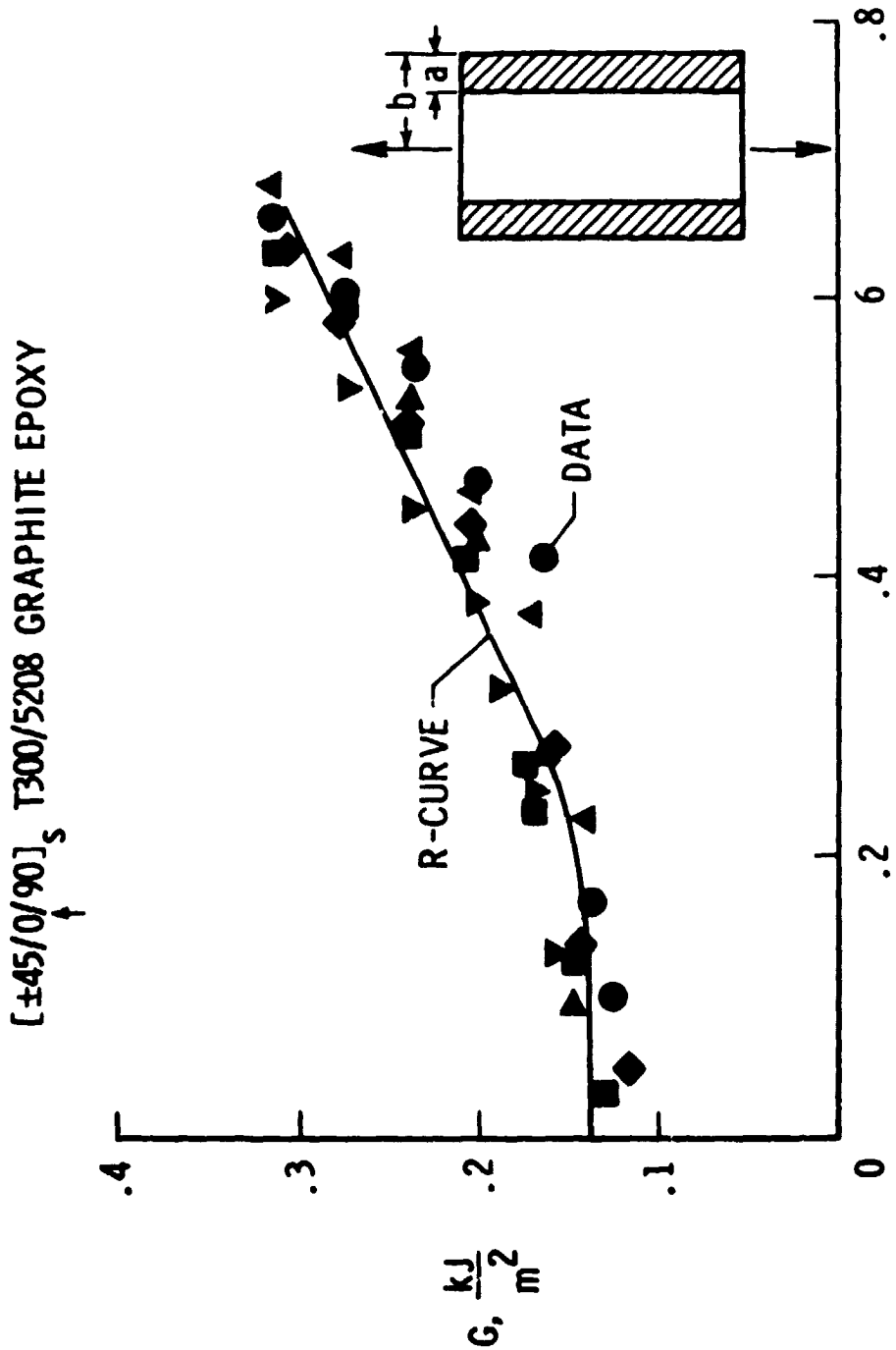

Fig 7 Delamination resistance curve

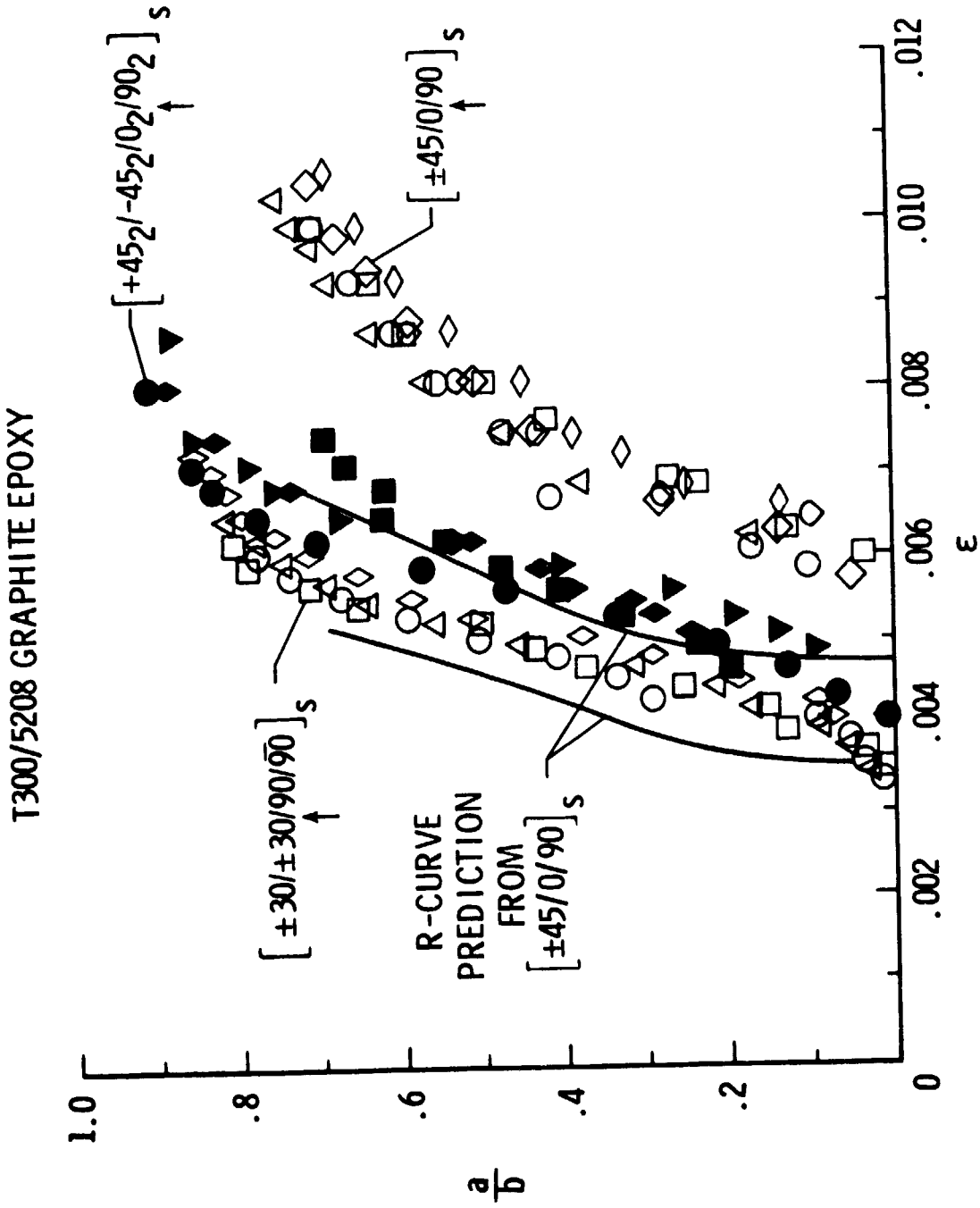

Fig 8 Prediction of stable delamination growth

$$G = \frac{P^2}{2b}\frac{dc}{da}$$

DOUBLE CANTILEVER BEAM

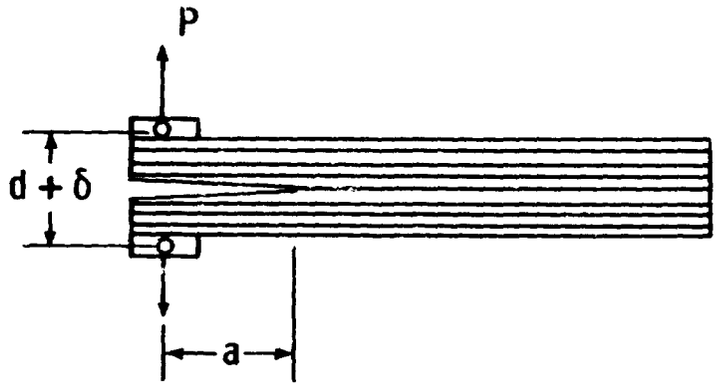

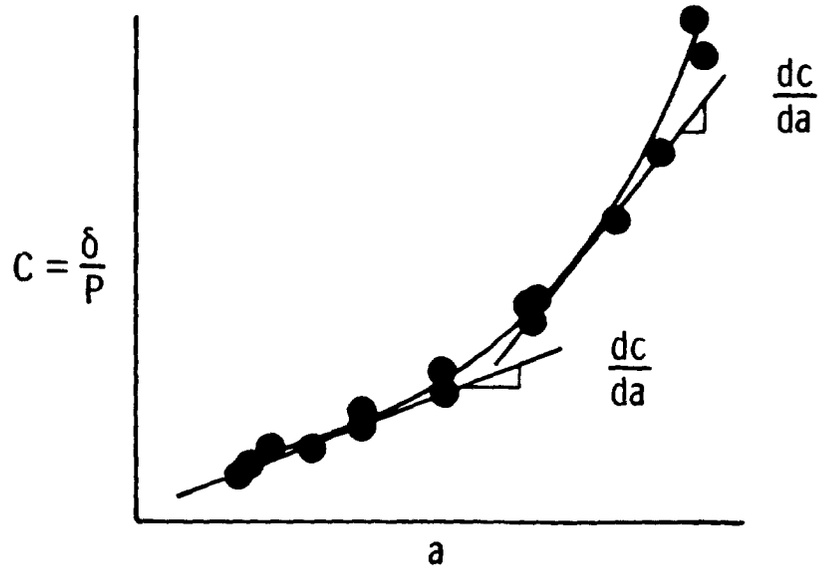

Fig 9 Double cantilever beam test for mode I interlaminar fracture toughness

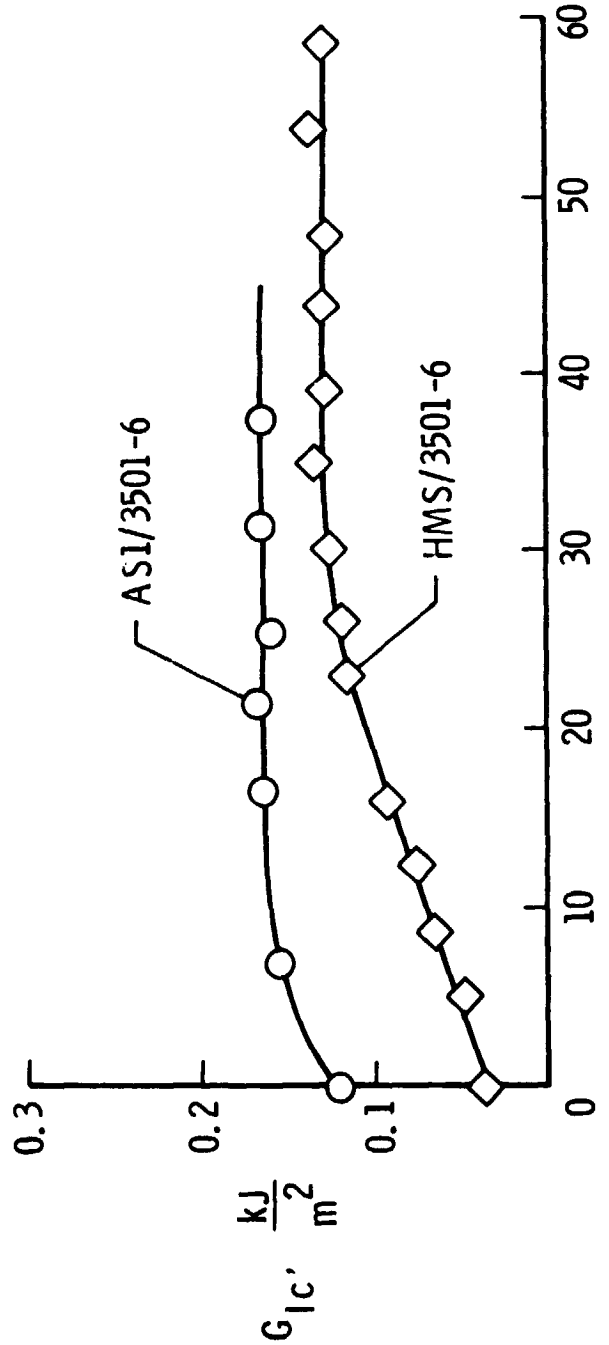

Fig 10 R-curves for delamination growth in unidirectional double cantilever beam specimens

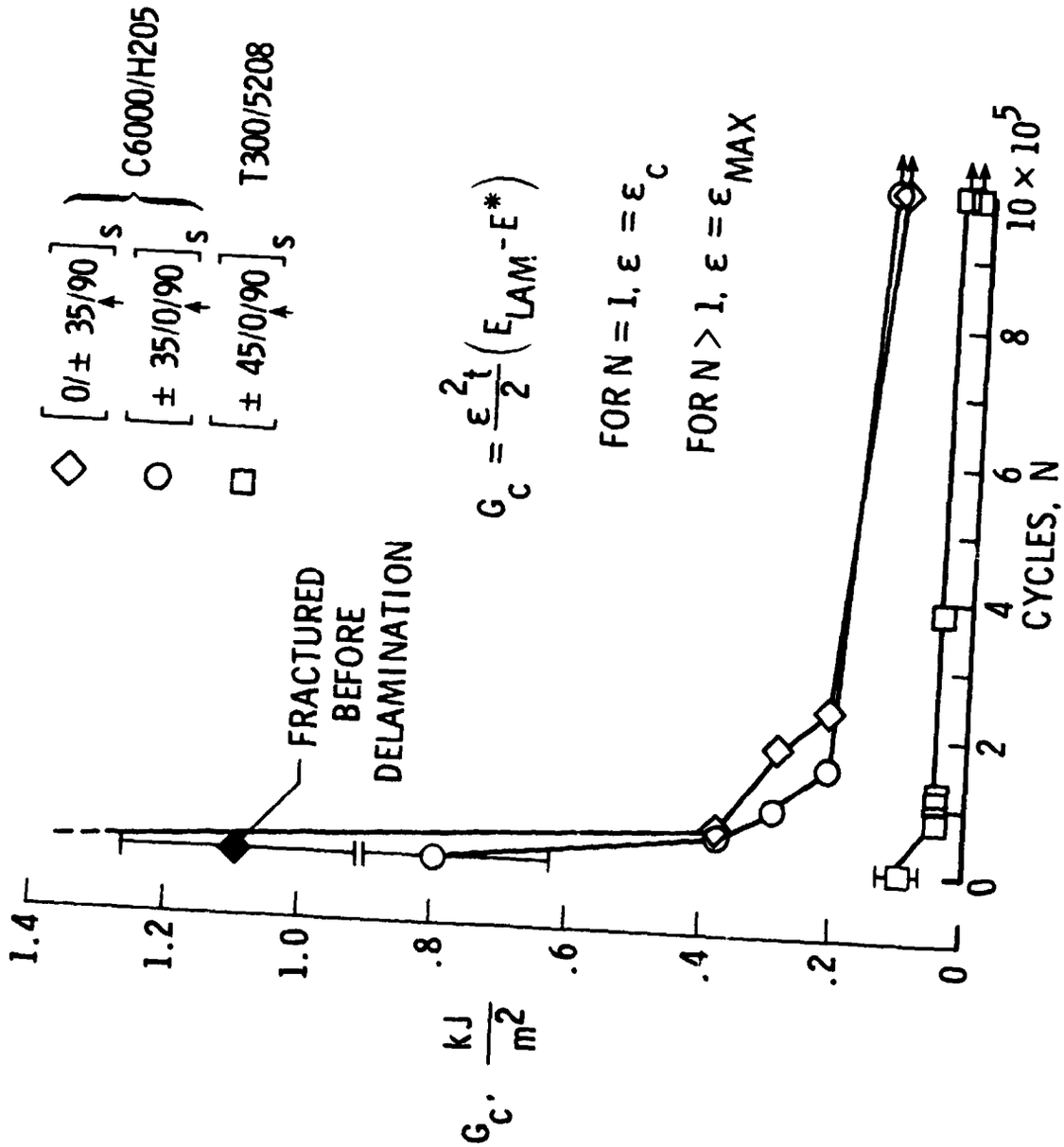

Fig 11 Interlaminar G_c as a function of fatigue cycles

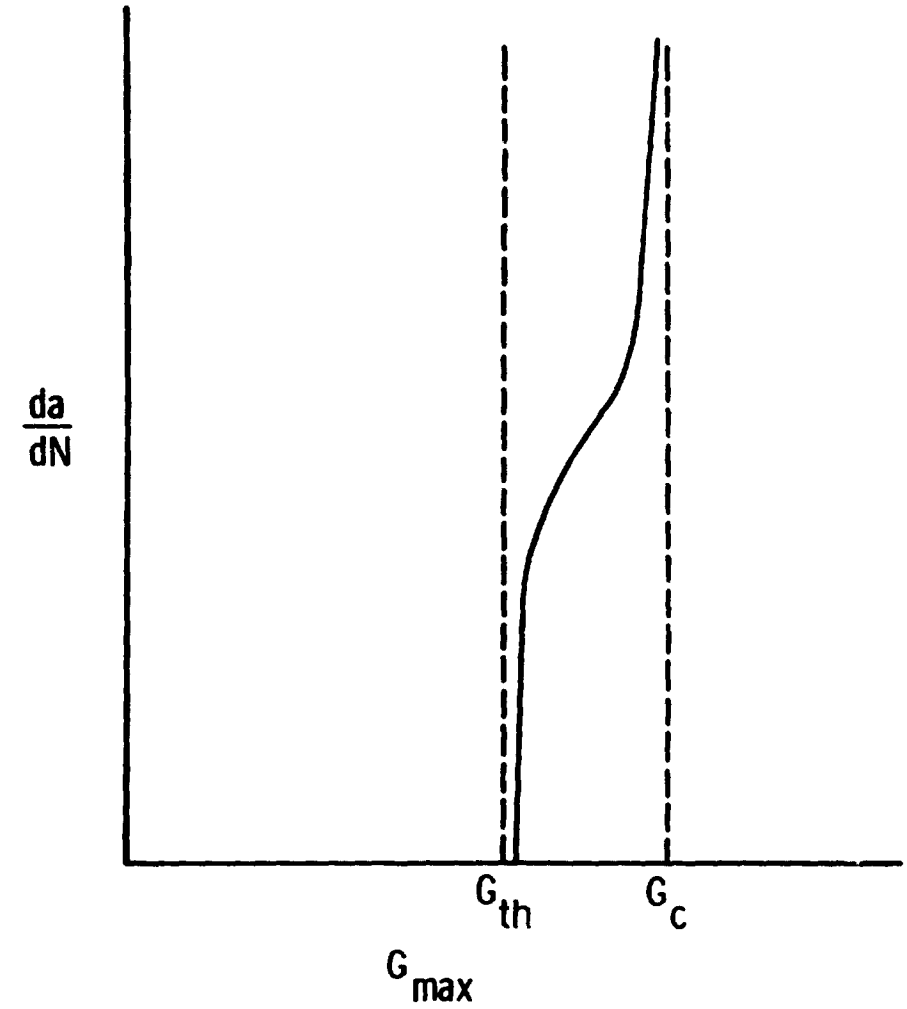

Fig 12 Schematic showing rate of delamination growth between fatigue threshold and static interlaminar fracture toughness

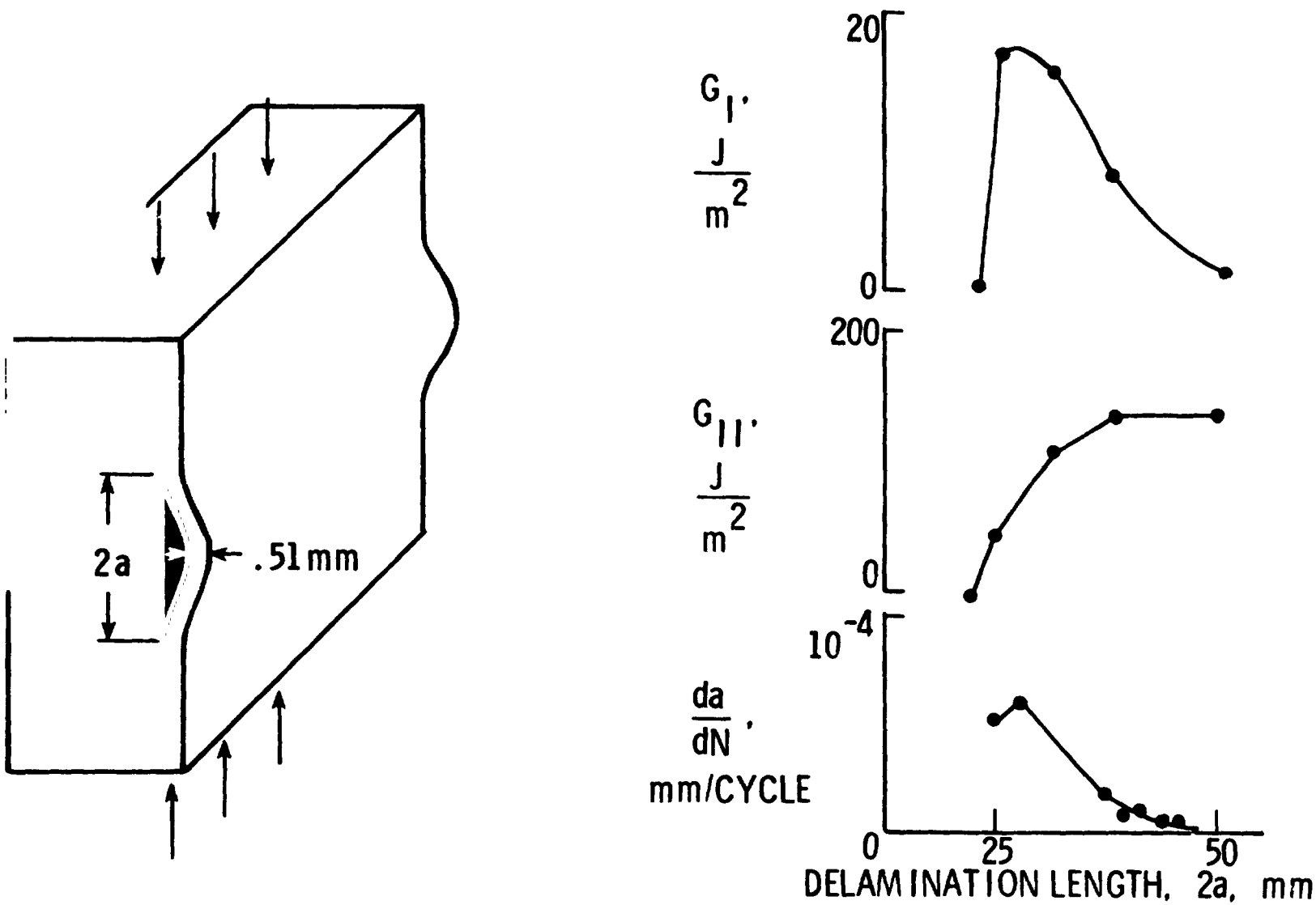

Fig 13 Strain energy release rate analysis of instability related delamination growth

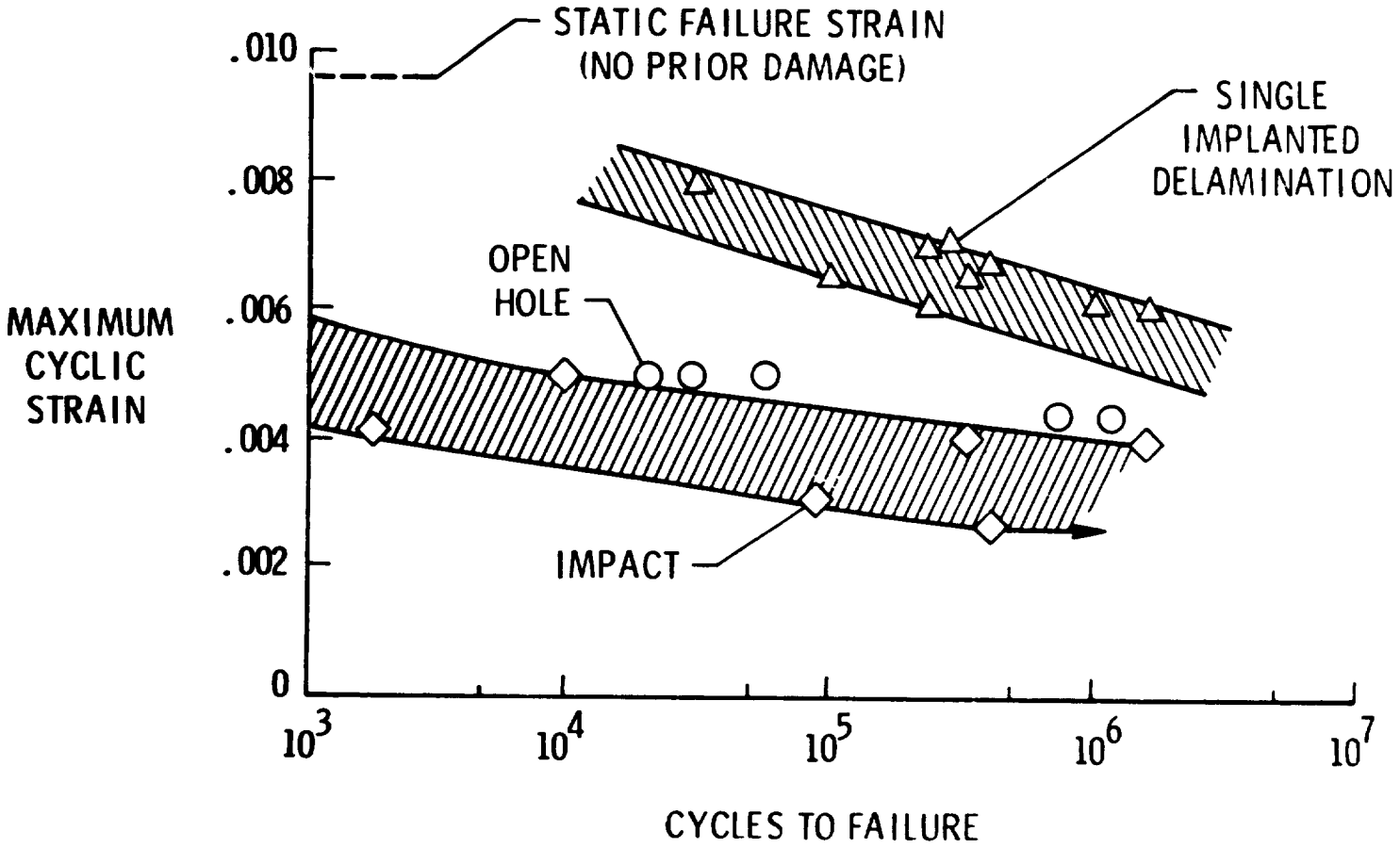

Fig 14 Cyclic compression fatigue life trends for T300/5208 graphite epoxy laminates

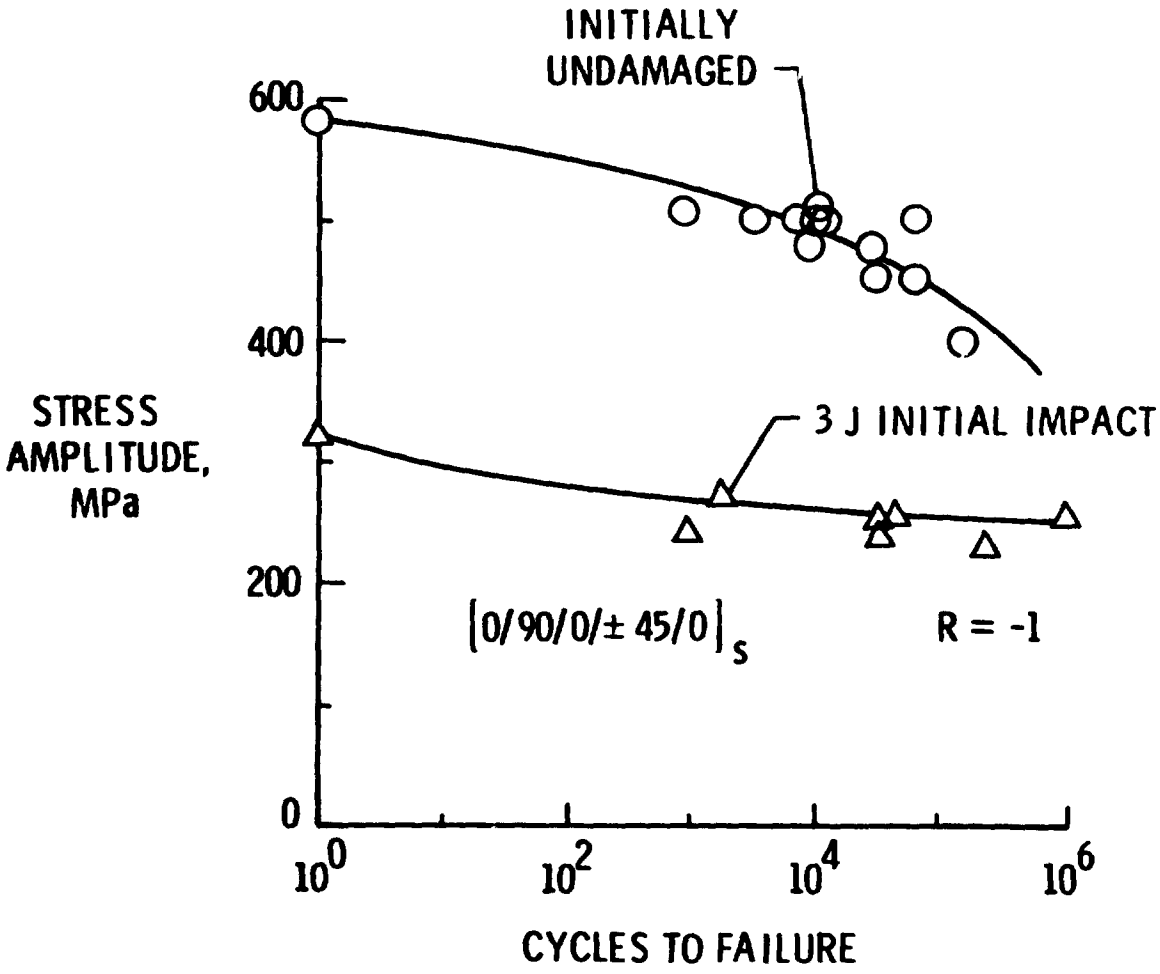

Fig 15 Fatigue behavior of initially undamaged and impacted graphite epoxy laminates under fully reversed cyclic loading

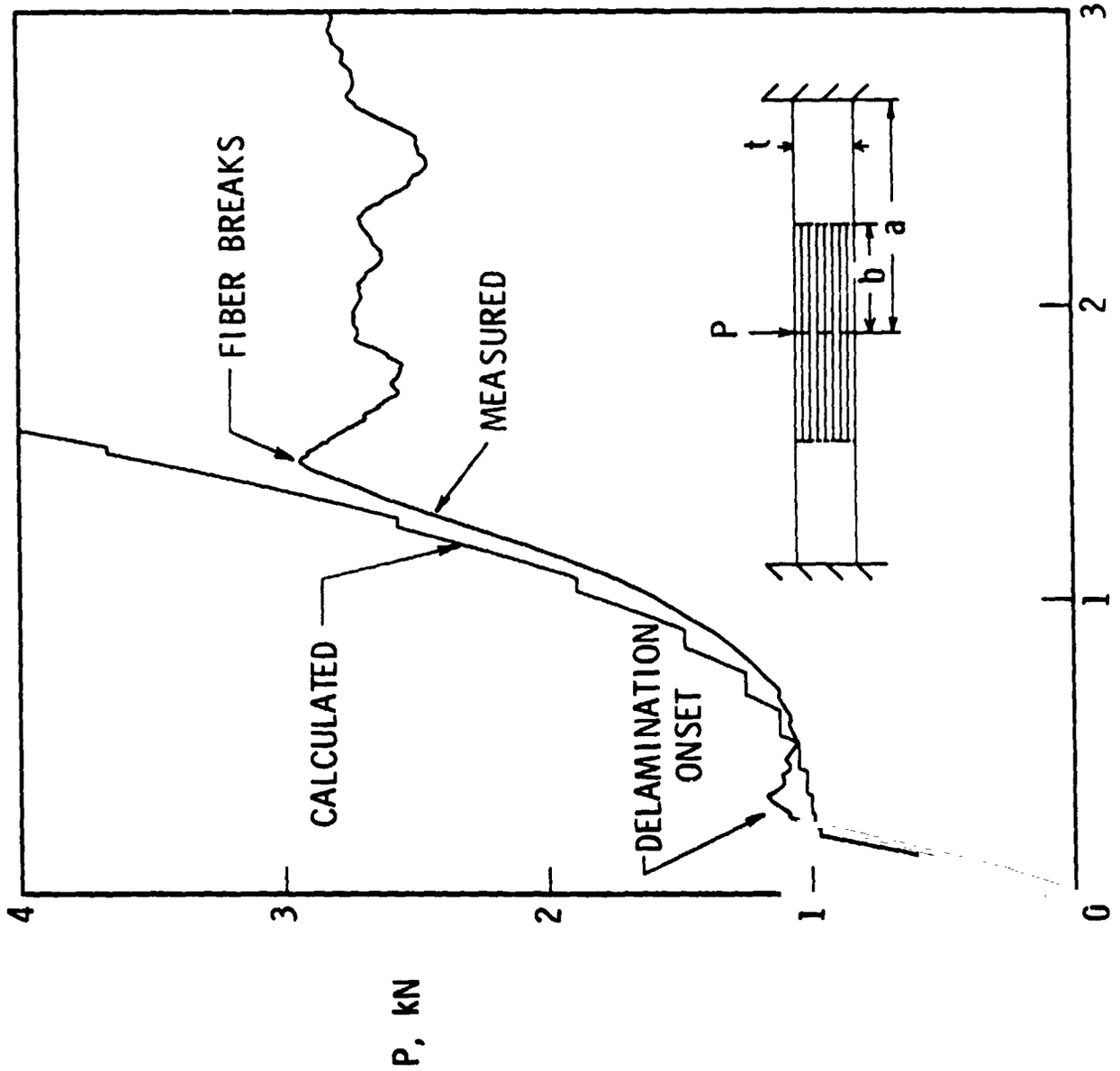

Fig 16 Prediction of multiple delamination growth due to out-of-plane loading

EIGHT-PLY $[\pm 35/0/90]_s$ LAMINATE

LAMINATE STIFFNESS; DELAMINATION ONSET

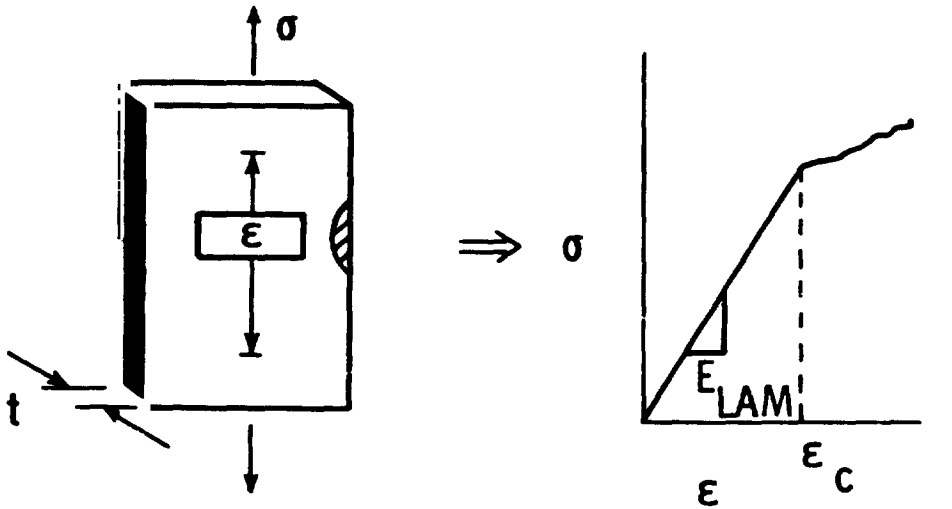

$\Rightarrow$ σ

$\Rightarrow$

INTERLAMINAR FRACTURE TOUGHNESS

$$G_c = \frac{\varepsilon_c^2 t}{2}\left(E_{LAM} - E^*\right)$$

SUBLAMINATE STIFFNESS

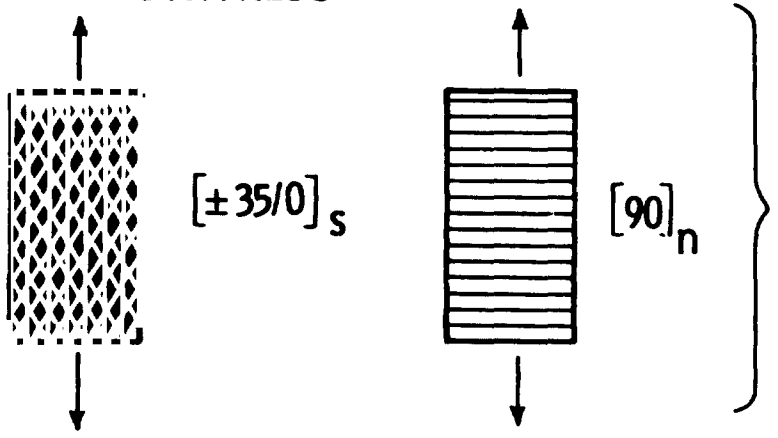

$$E^* = \frac{6E_{(\pm 35/0)_s} + 2E_{(90)_n}}{8}$$

Fig 17 Edge delamination test for mixed-mode interlaminar fracture toughness

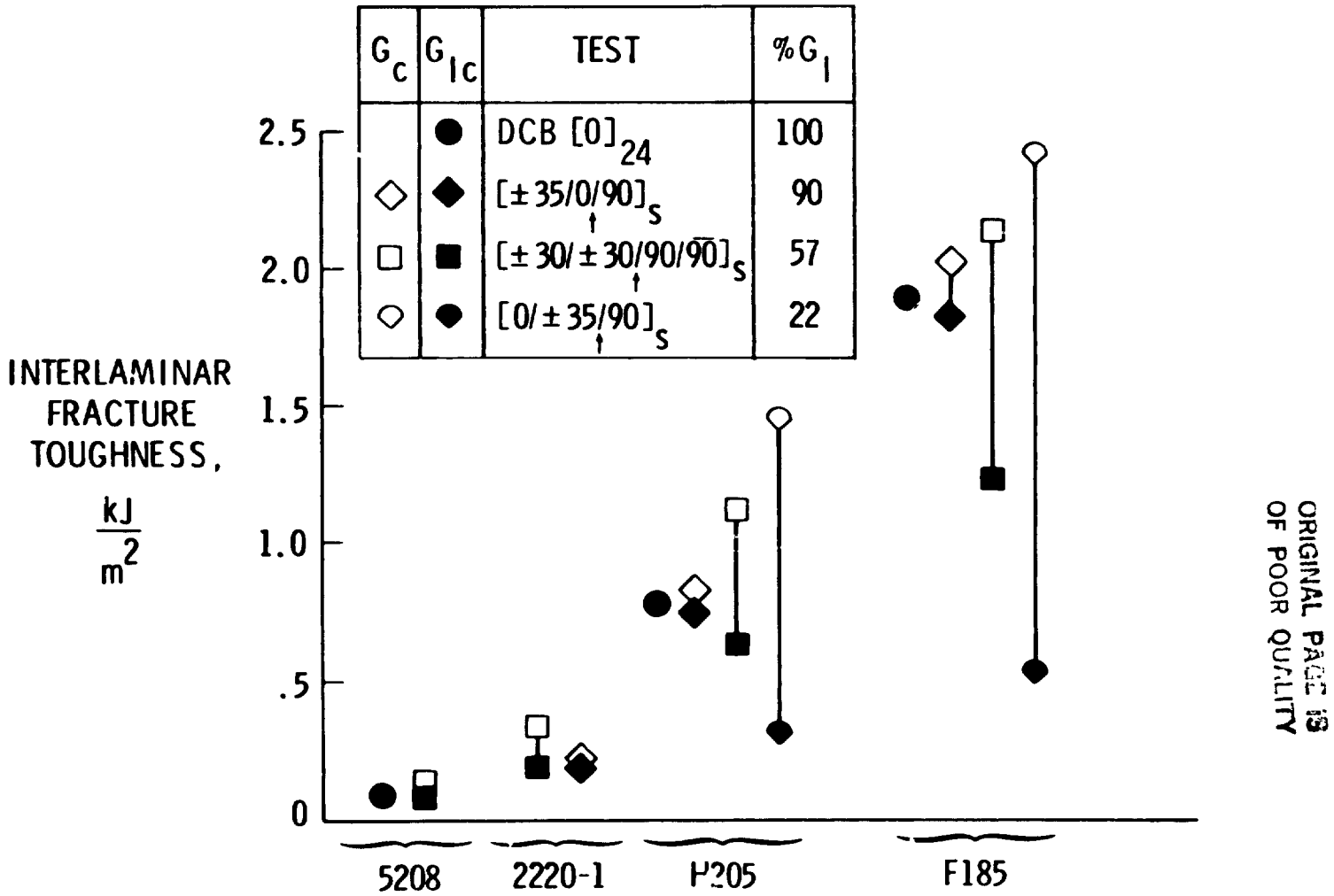

Fig 18 Interlaminar fracture toughness of graphite composites with different matrix resins